28 September 2001

ELSEVIER

Chemical Physics Letters 346 (2001) 123–128

CHEMICAL PHYSICS LETTERS

www.elsevier.com/locate/cplett

Influence of time delayed global feedback on pattern formation in oscillatory CO oxidation on Pt(1 1 0)

Michael Pollmann *, Matthias Bertram, Harm Hinrich Rotermund

Fritz–Haber-Institut der Max-Planck-Gesellschaft, Faradayweg 4-6, 14195 Berlin, Germany

Received 5 June 2001; in final form 2 August 2001

Abstract

Spatiotemporal pattern formation in the catalytic CO oxidation on Pt(1 1 0) is controlled by means of global delayed feedback applied through the gas phase. Using photoemission electron microscopy we have investigated the dynamical response of the system to a change of feedback intensity and time delay. Well defined synchronization and desynchronization regimes alternate when the delay is varied. In the case of synchronization the surface shows spatial homogeneous oscillations whereas in the case of desynchronization non-uniform patterns are observed. Furthermore two-phase clusters with period doubled local oscillations are studied. Phase balance between single cluster areas and breathing cluster modes are observed.

1. Introduction

The interplay of reaction and diffusion leads to pattern formation in reacting systems. An important goal is to find ways to control such chemical reactions. One possibility is to drive the reaction by an artificial force from the outside [1–4]. Another way, responding more directly to the dynamical behaviour of the studied system, is to use a feedback. Studies on feedback-induced reactions gained considerable interest both theoretically and experimentally [5–11]. Besides using a direct feedback loop, the signal can be delayed in time before it is fed back into the reaction-system [12–18]. To probe effects of global feedback on chemical patterns catalytic surface reactions are convenient systems because global feedback can be easily implemented via the gas phase. A change of pressure in the gas phase affects the reaction state on the whole active surface area.

Among surface chemical reactions pattern formation in the catalytic oxidation of carbon monoxide (CO) on a Pt(1 1 0) single crystal surface is best understood. Observed spatiotemporal patterns include rotating spiral waves, target patterns, standing waves, and turbulence [19,20]. Previous experiments revealed that global gas phase coupling has a significant effect on the dynamical behaviour of this and similar systems [21–25]. The artificial application of global feedback where control parameters can be systematically changed enables a more general study of possible effects of global coupling. Previously we have shown that in this system turbulence can be suppressed by means of global delayed feedback [11]. In this Letter we report on feedback-induced spatiotemporal patterns in the oscillatory CO oxidation in absence of

* Corresponding author. Fax: +49-30-8413-5128.

E-mail address: pollmann@fhi-berlin.mpg.de (M. Pollmann).

0009-2614/01/$ - see front matter
PII: S0009-2614(01)00936-8

turbulence. The effect of time delay is systematically investigated.

2. Method

The catalytic oxidation of CO on platinum proceeds via the Langmuir–Hinshelwood mechanism. Chemisorbed carbon monoxide and dissociatively adsorbed oxygen react to carbon dioxide, which immediately desorbs into the gas phase. Molecules of CO are diffusively mobile on the surface. Interaction between reaction and diffusion can lead to the formation of spatiotemporal patterns in the adsorbate coverage, which is visualized by means of photoelectron emission microscopy (PEEM) [26]. This method displays the local work function (φ) across a surface area. The work function is a direct consequence of the adsorbate coverages on the surface. By studying the local image brightness conclusions about the coverage can be deduced. Three different homogeneous adsorbate states exist, the clean Pt surface and the fully O- or CO-covered surfaces, respectively. The free surface has the lowest work function and is displayed as bright areas. Even brighter areas, which were found in earlier measurements and assigned to subsurface oxygen [27–29], were not observed in the measurements presented here. The O-covered regions with the highest work function ($\Delta\varphi = +0.8$ eV) show up as dark areas. The work function of a CO-covered ($\Delta\varphi = +0.3$ eV) surface lies in between – therefore the areas are grey. The instrument's field-of-view was chosen to be about 350 μm in diameter. The lateral resolution was typically 1 μm. The PEEM images were recorded on S–VHS tape using a standard video camera at a rate of 25 images/s.

The pressure gauges for O_2 and CO allowed controlled dosing of the reactants into the UHV chamber. The principal idea of the experiment is to control the actual dosing rate of CO by the real-time properties of the imaged concentration patterns. To generate the control signal the total inverted PEEM intensity $I(t)$, integrated over the whole image, is delayed by a time τ_d. The variation of the CO partial pressure in the chamber followed the temporal modulation of the dosing rate with an additional intrinsic delay determined by the residence time of gases in the pumped chamber. The controlled global feedback was introduced, such that $p_{CO}(t) = p_0 + \mu(I(t-\tau) - I_0)$, where p_0 is the CO partial pressure in the absence of feedback, the coefficient μ determines the feedback intensity, τ is the effective delay time, and I_0 is the average base level of the integral PEEM image intensity without feedback.

To minimize the effect of internal global coupling on the reaction dynamics about 80% of the Pt(1 1 0) single crystal surface (10 mm in diameter) was covered by microlithographic deposition with Ti. The Ti oxidized to TiO_2, which is inactive in the studied chemical reaction. Therefore only the free Pt areas remained active.

3. Results and discussion

The reaction parameters were chosen that in absence of feedback the system was in an oscillatory state. The sample showed at first homogeneous oscillations of a period of about 3.5 s, which then were successively replaced by stable rotating spirals or target patterns formed around defects.

First we present results of experiments where only the time delay was varied but the feedback intensity was kept constant at $\mu = 0.4 \times 10^{-5}$ mbar. The starting point for each measurement was an O-covered surface with oxygen continuously fed into the chamber. After setting a certain delay the CO valve was opened. The dynamical behaviour of the system was found to be strongly dependent on the time delay, see Fig. 1a.

For small delays between $\tau = 0.5$ and 2.8 s the system exhibits stable homogeneous oscillations. The same behaviour is observed for τ above 3.2 up to 5 s. The whole surface acts synchronous in the final state independent of the starting conditions. For delays lower than 0.5 s and between 2.8 and 3.2 s homogeneous oscillations are unstable. After a few minutes different patterns (spirals or islands) form and gradually displace the oscillating uniform state. This process can be described as desynchronization. In most experiments the forming patterns are clearly different as compared to the non-perturbed system (e.g., freely moving spirals

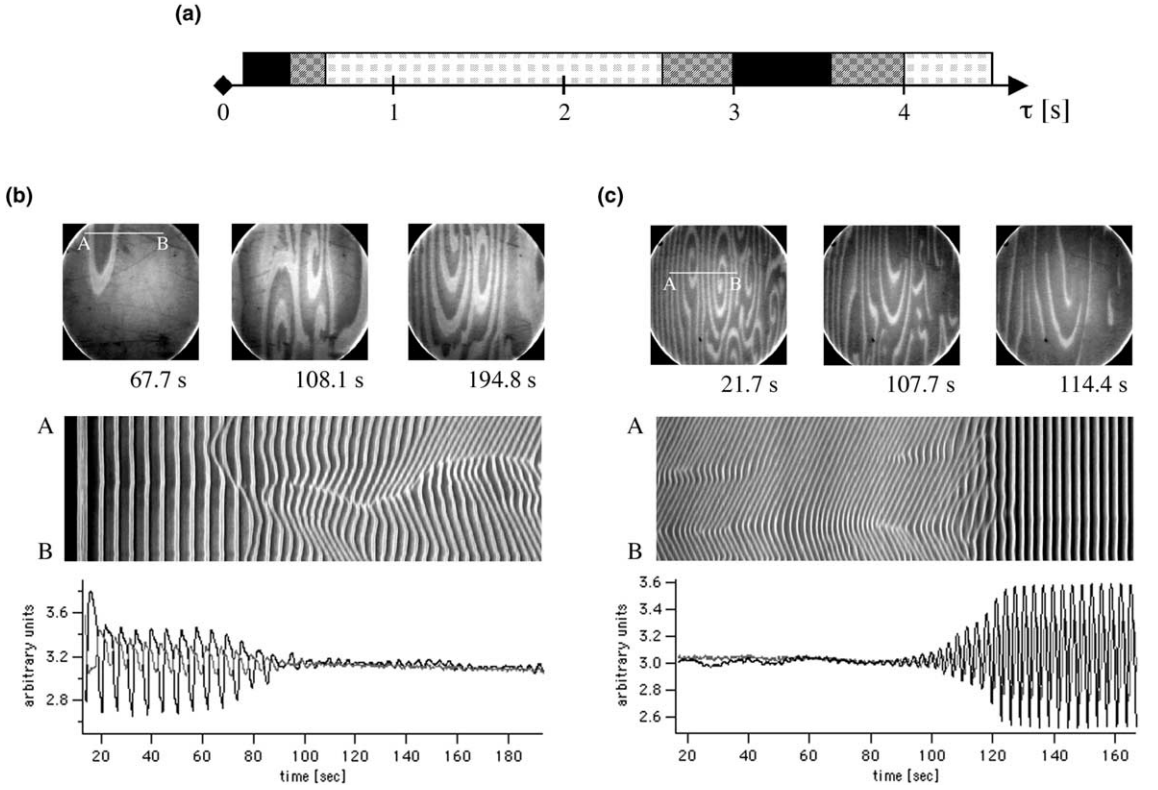

Fig. 1. System behaviour for constant feedback intensity and different time delays. The black regions correspond to desynchronization, slightly shaded white areas show the synchronization regimes, and in dark grey checkerboard areas both types of behaviour are possible. (b) and (c) Examples of the processes of desynchronization and synchronization, respectively ($T = 241$ °C, $p_{O_2} = 4.0 \times 10^{-4}$ mbar, $p_{CO} = 3.0 \times 10^{-5}$ mbar, $\mu = 0.4 \times 10^{-5}$ mbar, $\tau = 3.8$ s (b) and 0.7 s (c)). Top row: PEEM images at different time moments with a field-of-view of 350 μm in diameter. Middle row: space–time diagrams along the line AB indicated in the first images. Bottom row: temporal variations of the integrated PEEM signal (black line) and CO partial pressure (grey line); the time-scale is the same as in the space–time diagram.

instead of target patterns pinned to defects). The desynchronization windows shrink at higher feedback intensities and can even be totally suppressed. Examples of the desynchronization and synchronization process are displayed in Figs. 1b and c, respectively.

The time delay has a strong influence on the oscillation period as can be seen in Fig. 2. In case of desynchronization the period was extracted from the global data before the oscillation breakdown occurred. At first the period increases as the delay is increased. At the transition from desynchronization to synchronization at $\tau = 3.7$ s a discontinuous decrease of the period to one half of its previous value occurs. As a result of the change

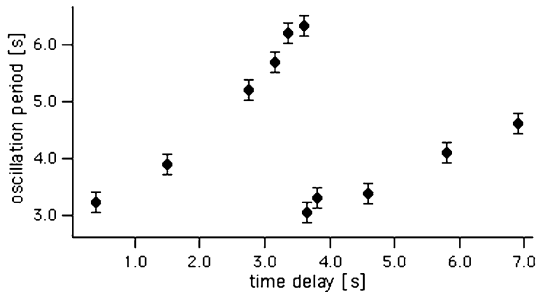

Fig. 2. Oscillation period of the forced system for different time delays. The rapid decrease of the period at $\tau = 3.7$ s marks the transition from desynchronization to synchronization ($\mu = 0.4 \times 10^{-5}$ mbar).

in the phase relation between global oscillation and feedback signal the transition between non-uniform and uniform spatial patterns takes place. Further increase of τ again results in an increase of the period.

Depending on whether the system is in the regime of synchronization or desynchronization changes in the feedback intensity have different impact on the system. In the synchronization regime non-uniform patterns are suppressed above intensities about 0.4×10^{-5} mbar and homogeneous oscillations occur (experiments were performed up to $\mu = 5.5 \times 10^{-5}$ mbar). The oscillation period showed no significant changes in this intensity range. The behaviour in the desynchronization regime was investigated for $\tau < 0.5$ s. Significant hysteresis effects are observed upon change of the feedback intensitiy. When μ was increased from low values the system showed at first non-uniform patterns and later homogeneous oscillations. Upon decreasing μ from high values three different dynamical regimes occur. As before homogeneous oscillations emerge for high intensities whereas non-uniform patterns occur for low μ. For intermediate intensity values cluster patterns arise (around $\mu \approx 3.5 \times 10^{-5}$ mbar). This type of pattern is not observed in measurements without feedback.

Fig. 3 shows an example of a typical cluster pattern. The surface splits into regions belonging to either one of two different cluster states that show antiphase oscillations (Fig. 3a). The single states exhibit period doubled oscillations; oscillation cycles of higher and lower amplitude alternate, see Fig. 3c. The two surface parts oscillate in phase with respect to the adsorbate state (e.g., the relative maxima in O-coverage coincide), but shifted by half a total period. During cluster for-

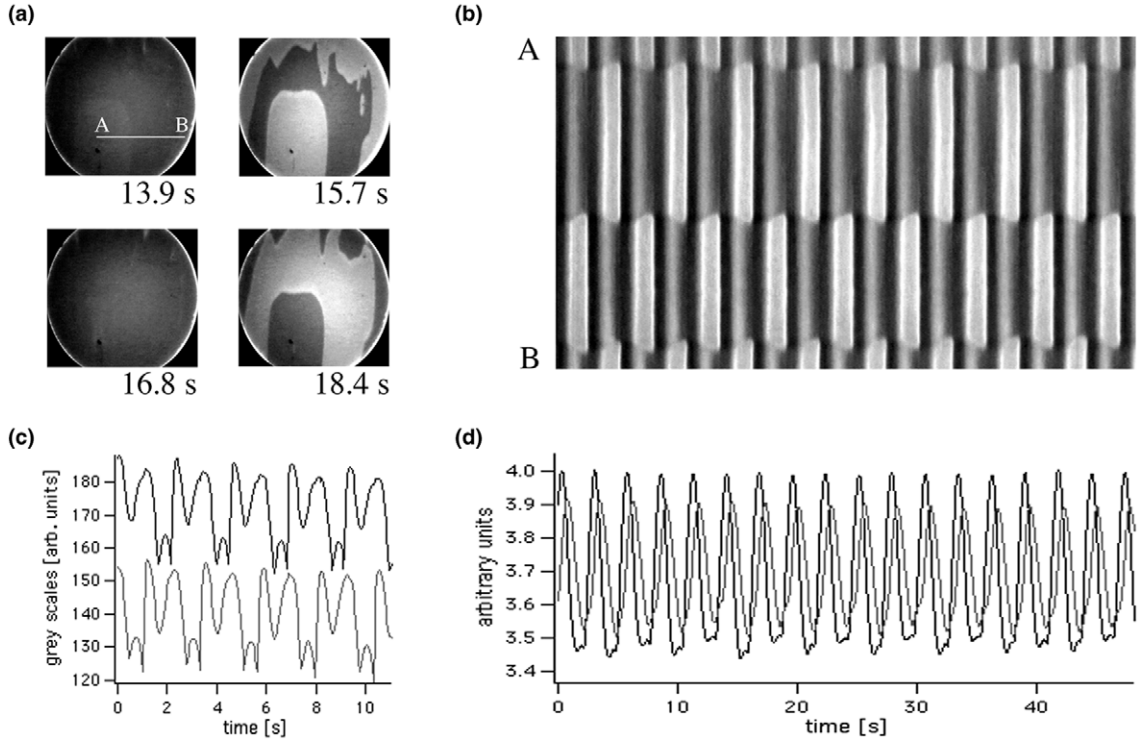

Fig. 3. Oscillatory cluster pattern ($T = 233$ °C; $p_{O_2} = 1 \times 10^{-4}$ mbar; $p_{CO} = 2.2 \times 10^{-5}$ mbar; $\tau = 0.45$ s; $\mu = 3.5 \times 10^{-5}$ mbar; field-of-view: 350 μm). (a) Typical PEEM images during one period. (b) Space–time plot along line AB indicated in the first PEEM image. (c) Temporal oscillations of the two cluster states. The grey line has been shifted downwards for clarity. (d) Temporal variations of the global PEEM intensity (black line) and CO partial pressure (grey line). The time-scale is the same as in (b).

mation a slow movement of the nodal lines between cluster areas occurs on a time-scale of many oscillation cycles. After this transient the area of the clusters is almost equally distributed; a state of phase balance is reached such that the local oscillations sum up to global oscillations of doubled frequency, see Fig. 3d. Additionally there exists a periodic 'breathing' of the nodal lines each cycle. During the mostly CO-covered state the bright areas expand at the expense of the grey areas until the system reaches the O-covered state. The strength of breathing depends on the oscillation period and, as feedback parameters are varied and the oscillation period changes, increases with increasing period. For long periods of several seconds we have observed a different type of clusters with pronounced movement of the nodal lines and continuous formation of new cluster islands, which was a transient to non-uniform patterns.

The spatial distribution of clusters does not change upon a change in feedback intensity or time delay. However, by increasing (decreasing) the intensity the oscillation amplitude and frequency increase (decrease). For sufficiently high μ clusters transform into uniform oscillations. When τ is increased the oscillation amplitude increases but the frequency decreases as in the case shown in Fig. 2.

At the end we discuss the experimental findings with respect to recent theoretical simulations addressed to the same problem [18]. Good agreement is found between our experiments and their simulations: synchronization and desynchronization regimes were predicted dependent on the chosen time delay. The formation of cluster patterns and their phase-balanced spatial distribution were also proposed. However period doubling of cluster oscillations was only observed when simulations started from a turbulent state [11].

4. Summary

This work presents experiments of time delayed feedback measurements of the oscillatory CO-oxidation on Pt(1 1 0). We focussed in this work on one hand on the dynamical behaviour of the system upon a change of the time delay. Well defined alternating synchronization and desynchronization regimes are found. In the case of synchronization the surface shows spatial homogeneous oscillations whereas in the case of desynchronization pattern formation occur. On the other hand we studied cluster patterns which can be described as period doubled two-phase clusters. They turned out to be similar to clusters in the light sensitive Belousov–Zhabotinsky reaction influenced by global, non-delayed feedback [9]. We were able to show that the specific choice of feedback parameters allows an efficient control over pattern formation in the studied system.

Acknowledgements

We gratefully acknowledge the support of the DFG through SFB 555 'Complex nonlinear systems'.

References

[1] P. Coullet, K. Emilsson, Physica D 61 (1992) 119.
[2] M. Braune, H. Engel, Chem. Phys. Lett. 211 (1993) 534.
[3] A. Schrader, M. Braune, H. Engel, Phys. Rev. E 52 (1995) 98.
[4] A.L. Lin, M. Bertram, K. Martinez, H.L. Swinney, A. Ardelea, G.F. Carey, Phys. Rev. Lett. 84 (2000) 4240.
[5] S. Grill, V.S. Zykov, S.C. Müller, Phys. Rev. Lett. 75 (1995) 3368.
[6] V. Petrov, S. Metens, P. Borckmans, G. Dewel, K. Showalter, Phys. Rev. Lett. 75 (1995) 2895.
[7] Th. Pierre, G. Bonhomme, A. Atipo, Phys. Rev. Lett. 76 (1996) 2290.
[8] M. Braune, H. Engel, Phys. Rev. E 62 (2000) 5986.
[9] V.K. Vanag, L. Yang, M. Dolnik, A.M. Zhabotinsky, I.R. Epstein, Nature 406 (2000) 389.
[10] L. Yang, M. Dolnik, A.M. Zhabotinsky, I.R. Epstein, Phys. Rev. E 62 (2000) 6414.
[11] M. Kim, M. Bertram, M. Pollmann, A.S. Mikhailov, H.H. Rotermund, G. Ertl, Science 292 (2001) 1357.
[12] D. Battogtokh, A.S. Mikhailov, Physica D 90 (1996) 84.
[13] W. Lu, D. Yu, R.G. Harrison, Phys. Rev. Lett. 76 (1996) 3316.
[14] G. Franceschini, S. Bose, E. Schöll, Phys. Rev. E 60 (1999) 5426.
[15] M.Y. Choi, H.J. Kim, D. Kim, H. Hong, Phys. Rev. E 61 (2000) 371.
[16] A. Takamatsu, T. Fujii, I. Endo, Phys. Rev. Lett. 85 (2000) 2026.

[17] G. Kozyreff, A.G. Vladimirov, P. Mandel, Phys. Rev. Lett. 85 (2000) 3809.
[18] M. Bertram, A.S. Mikhailov, Phys. Rev. E 63 (2001) 066102.
[19] S. Jakubith, H.H. Rotermund, W. Engel, A. von Oertzen, G. Ertl, Phys. Rev. Lett. 65 (1990) 3013.
[20] R. Imbihl, G. Ertl, Chem. Rev. 95 (1995) 697.
[21] M. Ehsasi, O. Frank, J.H. Block, K. Christmann, Chem. Phys. Lett. 165 (1990) 115.
[22] R. Imbihl, G. Veser, J. Vac. Sci. Technol. A 12 (1994) 2170.
[23] M. Falcke, H. Engel, Phys. Rev. E 50 (1994).
[24] M.A. Liauw, P.J. Plath, N.I. Jaeger, J. Chem. Phys. 104 (1996) 6375.
[25] K.C. Rose, D. Battogtokh, A. Mikhailov, R. Imbihl, W. Engel, A.M. Bradshaw, Phys. Rev. Lett. 76 (1996) 3582.
[26] H.H. Rotermund, Surf. Sci. Rep. 29 (1997) 265.
[27] J. Lauterbach, K. Asakura, H.H. Rotermund, Surf. Sci. 313 (1994) 52.
[28] A. von Oertzen, A. Mikhailov, H.H. Rotermund, G. Ertl, Surf. Sci. 350 (1996) 259.
[29] A. von Oertzen, H.H. Rotermund, G. Ertl, A.S. Mikhailov, J. Phys. Chem. B 104 (2000) 3155.